

Photoproduction of η mesons off protons for $0.75 \text{ GeV} < E_\gamma < 3 \text{ GeV}$

V. Credé¹, O. Bartholomy¹, A. Anisovich¹, G. Anton², R. Bantes³, Yu. Beloglazov⁴, R. Bogendörfer², A. Ehmanns¹, J. Ernst¹, I. Fabry¹, H. Flemming⁵, A. Fösel², H. Freiesleben⁶, M. Fuchs¹, Ch. Funke¹, R. Gothe³, A. Gridnev⁴, E. Gutz¹, St. Höfgen³, I. Horn¹, J. Hößl², R. Joosten¹, J. Junkersfeld¹, H. Kalinowsky¹, F. Klein³, E. Klemp¹, H. Koch⁵, M. Konrad³, B. Kopf^{5,6}, B. Krusche⁷, J. Langheinrich³, H. Löhner⁹, I. Lopatin⁴, J. Lotz¹, H. Matthäy⁵, D. Menze³, J. Messchendorp⁸, C. Morales³, D. Novinski⁴, M. Ostrick³, H. van Pee¹, A. Radkov⁴, J. Reinhardt¹, S. Sack⁸, A. Sarantsev¹, S. Schadmand⁸, C. Schmidt¹, H. Schmieden³, B. Schoch³, G. Soft², V. Sumachev⁴, T. Szczepanek¹, U. Thoma¹, D. Walther³ and Ch. Weinheimer¹

(The CB-ELSA Collaboration)

¹ Helmholtz-Institut für Strahlen- und Kernphysik, Universität Bonn

² Physikalisches Institut, Universität Erlangen

³ Physikalisches Institut, Universität Bonn

⁴ Petersburg Nuclear Physics Institute, Gatchina, Russia

⁵ Institut für Experimentalphysik I, Ruhr-Universität Bochum

⁶ Institut für Kern- und Teilchenphysik, Universität Dresden

⁷ Physikalisches Institut, Universität Basel

⁸ Physikalisches Institut, Universität Giessen and

⁹ KVI, Groningen

(Dated: 30th December 2019)

Total and differential cross sections for the reaction $p(\gamma, \eta)p$ have been measured for photon energies in the range from 750 MeV to 3 GeV. The low-energy data are dominated by the $N(1535)S_{11}$ for which we determine $(M, \Gamma) = (1505 \pm 12, 152 \pm 15)$ MeV. Six nucleon resonances are observed in their decay into $p\eta$. At medium energies we find evidence for a new resonance $N(2080)D_{15}$ with $(M, \Gamma) = (2079 \pm 40, 368_{-50}^{+100})$ MeV. At γ energies above 1.5 GeV, a strong peak in forward direction develops, signalling the exchange of vector mesons in the t channel.

PACS numbers: PACS: 14.20

The study of baryon resonances, of their masses, widths and decay modes, is a prerequisite to improve our understanding of the internal structure of protons and neutrons. Apart from the recently suggested exotic $\Theta^+(1540)$ and $\Xi^{--}(1862)$ pentaquark states [1, 2, 3, 4, 5], the pattern of known baryon resonances listed by the Particle Data Group (PDG) [6] is, in the mass range below 1.8 GeV, generally well reproduced by present quark model calculations [7, 8, 9]. Above this mass, models predict many more resonances than have been seen experimentally. Moreover, the mass predictions of models using one-gluon exchange [7] or instanton-induced interactions [9] no longer agree. Lattice gauge calculations of ground-state baryons reproduce the masses rather well [10]. Even first excited states have been simulated on a lattice [11] but the baryon structure is still far from being understood.

Baryon resonances have large, overlapping widths rendering difficult the study of individual states, in particular of those which are only weakly excited. This problem can partly be overcome by looking at specific decay channels. The η meson, e.g., has isospin $I = 0$, and isospin conservation guarantees that the $N\eta$ final state can only be reached via formation of N^* resonances while contributions from Δ^* resonances are excluded. This is partic-

ularly helpful for coupled-channel analyses. Resonances observed in $N\pi$ or $N\pi\pi$ could belong to the N^* or Δ^* series, however, a coupling to the $N\eta$ channel identifies them as N^* resonances.

In the near-threshold region, the η -production process is strongly dominated by a single resonance, $N(1535)S_{11}$. This resonance has continued to provoke many theoretical debates due to its unusual parameters. The branching ratio for $N(1535)S_{11} \rightarrow \eta N$ ($\approx 50\%$) is much larger than for any other nucleon resonance. As a consequence, even the very nature of the $N(1535)S_{11}$ as an excited nucleon has been questioned [12]. Precise data on the shape of the $N(1535)S_{11}$ resonance and of its photo-coupling should help to elucidate its nature. At present, the Particle Data Group gives a range from 100 to 200 MeV [6] for its width. Clearly, high-statistics data covering a wide range of photon excitation energies are needed to define the properties of the $N(1535)S_{11}$ more precisely and to identify contributions from other resonances to the $N\eta$ channel. At higher energies, it is expected that not only s -channel processes contribute to η production but also t - and u -channel exchange which may change the differential cross sections and, thus, mimic resonant contributions if not properly identified.

In this letter, we present total and differential cross

sections for the reaction

$$\gamma p \rightarrow p\eta ; \quad \eta \rightarrow \gamma\gamma \text{ and } \eta \rightarrow 3\pi^0 \rightarrow 6\gamma \quad (1)$$

covering the entire resonance region and, thus, extending the already existing database [14, 15, 16, 17, 18].

The experiment (Fig. 1) was carried out at the tagged photon beam of the **E**lectron **S**tretcher **A**ccelerator (ELSA) of the University of Bonn. Electrons were extracted at energies of 1.4 and 3.2 GeV, covering photon energies from 300 MeV to 3.0 GeV, with a typical intensity of $1\text{--}3 \times 10^6$ photons/s. The photon beam hit a liquid H₂ target of 5 cm length and 3 cm diameter. Charged reaction products were detected in a 3-layer scintillating fiber (scifi) detector. One of the layers was straight, the fibers of the other two layers encircled the target with $\pm 25^\circ$ with respect to the first layer so that the intersection point of a proton could be reconstructed for polar angles from 15° to 165° . Charged particles and photons were detected in the Crystal Barrel detector [19]. It consisted of 1380 CsI(Tl) crystals with photodiode readout covering 98% of 4π . A total absorption γ detector (an oil Čerenkov counter with 6 segments) placed downstream determined the photon flux.

The coincidence between tagger and scifi detector provided the first-level trigger of the experiment. From the hit pattern in the Crystal Barrel detector, a fast cluster logic determined the number of 'particles' defined by clusters of contiguous crystals with individual energy deposits above 15 MeV. A second level trigger was generated for events with two or more 'particles' in the cluster logic.

In the data analysis, clusters with two local maxima were split into two 'particles' sharing the total energy deposit. The offline threshold for accepted particles was set to 20 MeV. Protons needed energies above 35 MeV to traverse the inner two scifi layers and, thus, to produce a trigger. A proton kinetic energy of 90 MeV was needed to reach the barrel calorimeter and to deposit the minimum cluster energy of 20 MeV.

In the first step of data reduction, we required that all photons from one of the reactions (1) were detected in the Crystal Barrel and that not more than one candidate for the proton was found. Thus, we retained events with 2, 3, 6 or 7 'particles'. Proton candidates were identified by the geometrical relation of impact points in the

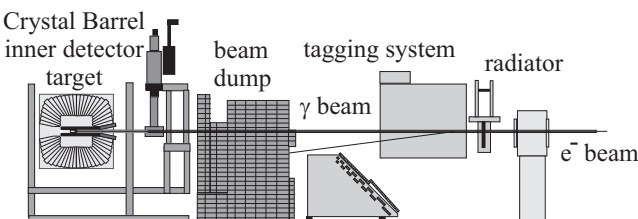


Figure 1: Experimental setup at ELSA in Bonn

scifi and in the barrel. In the further analysis, protons were not used but treated as missing particles. The remaining 'particles' are treated as photons. The events were then subjected to kinematic fits imposing energy and momentum conservation. Events with two photons were fitted to the $p(\gamma, \gamma\gamma)p_{\text{missing}}$ hypothesis using one constraint, those with 6 photons to $p(\gamma, 3\pi^0)p_{\text{missing}}$ (four constraints).

Fig. 2 shows the $\gamma\gamma$ invariant mass spectrum after a 10^{-4} confidence level cut in the kinematic fit. The π^0 and η meson (also shown in inset (a)) are observed above a small residual background. Inset (b) shows the resulting $3\pi^0$ invariant mass spectrum, again above some small background (10^{-2} confidence level cut). In a final step, the mass of the η was imposed in a $\gamma p \rightarrow p\eta \rightarrow p2\gamma$ two-constraint kinematic fit. The residual background events under the $\eta_{3\pi^0}$ as well as under the $\eta_{\gamma\gamma}$ peaks were subtracted using side bins. On the average, there were 1–4 background events per measured bin.

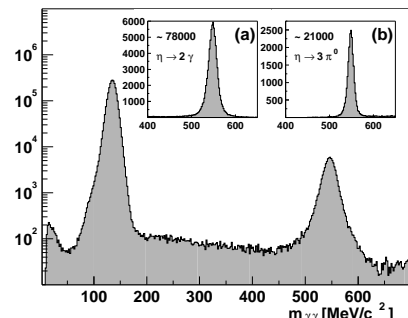


Figure 2: The two- γ invariant mass spectrum from events with two photons detected, after a kinematic fit to $\gamma p \rightarrow p\gamma\gamma$. Notice the logarithmic scale! Inset (a) shows an expanded view of the η region; (b) events with η decaying into $3\pi^0$.

The acceptance of the detector was determined from GEANT-based Monte Carlo simulations. In the center-of-mass system, the acceptance vanishes for forward protons leaving the Crystal Barrel through the forward hole, and for backward protons having very low lab momenta.

The shape of our measured differential cross sections for π^0 production [20] agrees very well with SAID [21] and we used these for normalization. Due to uncertainties in the determination of the photon flux, energy-dependent scaling factors were used for the absolute normalization of the 1.4 GeV data set. The 3.2 GeV data set required an overall scaling factor of 0.75 applied to the measured photon flux. We estimate a normalization error of our cross sections of $\pm 5\%$ and $\pm 15\%$, respectively.

Fig. 3 shows the differential cross sections from all four data sets (2, 3, 6, 7 'particles') combined. The ratio $\eta \rightarrow 2\gamma$ to $\eta \rightarrow 3\pi^0$ was determined for each bin in Fig. 3 and histogrammed, giving $\Gamma_{\eta \rightarrow 3\pi^0}/\Gamma_{\eta \rightarrow 2\gamma} = 0.826 \pm 0.004_{\text{stat}} \pm 0.003_{\text{syst}}$. This value reproduces the PDG value and demonstrates the good understanding of the detector response. At the same time, it justifies to

average the data from $\eta \rightarrow 2\gamma$ and $\eta \rightarrow 3\pi^0 \rightarrow 6\gamma$.

The bars in Fig. 3 represent the statistical errors, the bands below the cross sections the systematic errors evaluated by changing, in the Monte Carlo simulation, the beam axis ($= z$) with respect to the barrel axis by ± 3 mm, the position of the target centre along z by ± 1.5 mm, and the thickness of material between target and inner detector by ± 1 mm of Kapton foil. These contributions, and a $\pm 5\%$ error assigned to the reconstruction efficiency, are added quadratically.

The overall consistency with data from GRAAL [17] as well as from CLAS [18] is very good. At $E_\gamma \sim 1.1$ GeV ($W \sim 1716$ MeV/c 2), there is a small discrepancy between those two data sets, particularly visible in the total cross section (Fig. 4). We emphasize that our data cover a larger solid angle and a wider energy range; they do not suffer from instrumental background. At ~ 750 MeV, our detection efficiency for events with low-energy protons in the backward direction suffers from a large systematic error. For photon energies below 1.3 GeV, the data are well reproduced by SAID [21] and MAID [22]. Above, small deviations between data and SAID show up which become increasingly important at higher energies.

The data are interpreted in an isobar model [13]. We include the Mainz–TAPS data [14] on η photoproduction to cover the threshold region, the beam asymmetry measurements from GRAAL [23] and our own data on $\gamma p \rightarrow p \pi^0$ [20]. Resonances are described by relativistic Breit–Wigner amplitudes except for the two S_{11} resonances at 1535 and 1650 MeV for which we use a three-channel K–matrix (π^0, η). The background is described by a reggeized t –channel ρ – ω exchange and by nucleon exchange in the s – and u –channel. Here we present the results on the $p\eta$ channel.

Table I: Masses and widths of $p\eta$ resonances.

N^*	M (MeV)	Γ (MeV)	$A_{3/2}/A_{1/2}$	$P_{in/out}$
$N(1520)D_{13}$	1530 ± 7	102 ± 15	< -2.4	$0.027^{+0.015}_{-0.010}$
PDG	1520^{+10}_{-5}	120^{+15}_{-10}	-6.9 ± 2.6	< 0.07
$N(1535)S_{11}$	1505 ± 12	152 ± 15		1
PDG	1505 ± 10	170 ± 80		1
$N(1650)S_{11}$	1626 ± 10	188 ± 30		$0.2^{+0.06}_{-0.07}$
PDG	1660 ± 20	160 ± 10		$0.01 - 0.4$
$N(1680)F_{15}$	1673 ± 8	98 ± 17	large	0.009 ± 0.007
PDG	1680^{+10}_{-5}	130 ± 10	-8.9 ± 3.6	< 0.05
$N(1720)P_{13}$	1734 ± 23	275^{+70}_{-40}	$-4.5^{+1.7}_{-2.5}$	$0.2^{+0.28}_{-0.10}$
PDG	1720^{+30}_{-70}	250 ± 50	-1.1 ± 2.1	< 0.1
$N(2080)D_{15}$	2079 ± 40	368^{+100}_{-50}	-0.5 ± 0.3	0.20 ± 0.03

The best fit gives χ^2 contributions from the Mainz–TAPS data of $\chi^2 = 182$ for 100 data points, and the GRAAL data of $\chi^2 = 97/51$. The differential cross sections of Fig. 3 contribute $\chi^2 = 676/630$. The fit uses 6 N^* resonances coupling to $N\eta$; the fit results are presented in Table I. We include the ratio of the helicity amplitudes

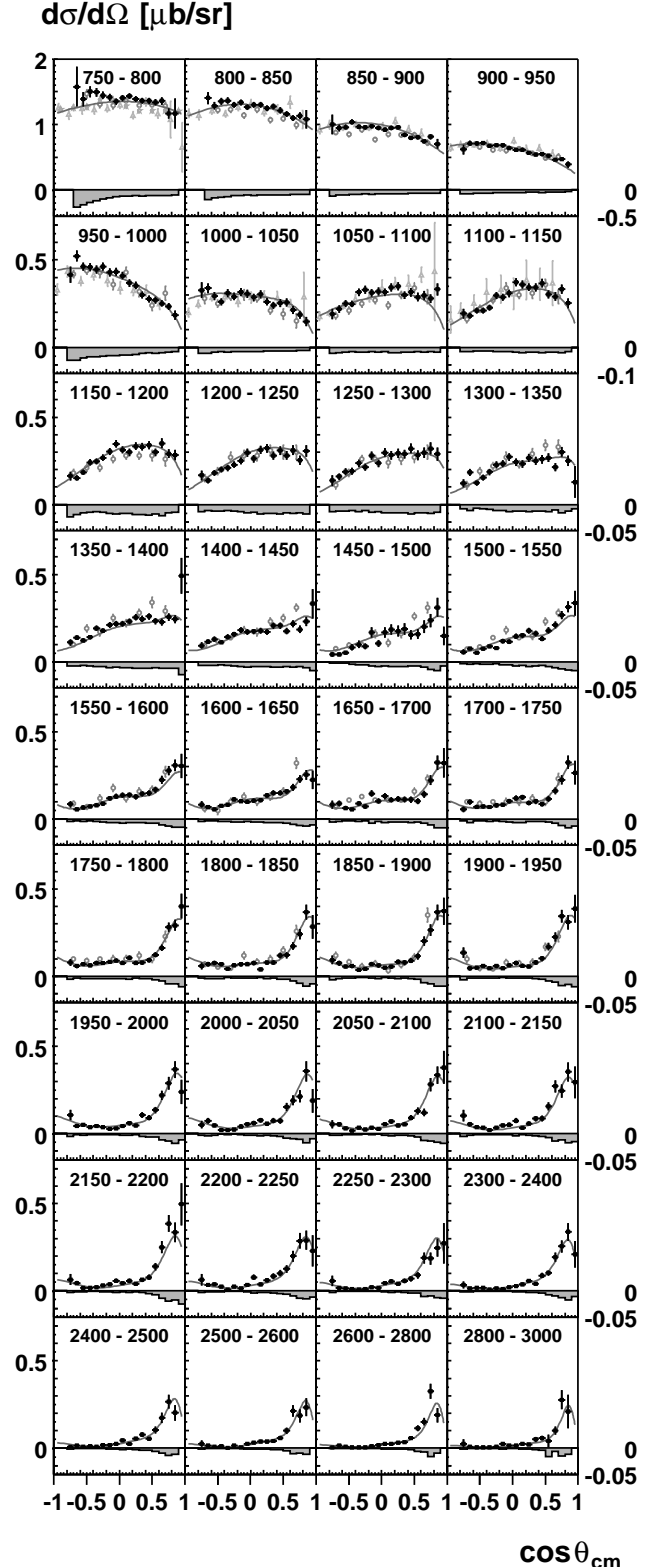


Figure 3: Differential cross sections for the reaction $\gamma p \rightarrow p\eta$. Experimental data for $E_\gamma = 750$ MeV to 3000 MeV: this work (black dots), TAPS, GRAAL and CLAS data (in light gray). The solid line represents our isobar fit. Systematic errors are shown as bands beneath cross sections. The overall normalization error, 5% below 1.3 GeV and 15% above, is not shown.

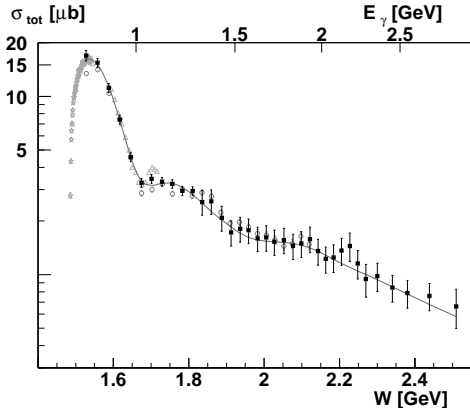


Figure 4: Total cross section (logarithmic scale) for the reaction $\gamma p \rightarrow p \eta$. See caption of Fig. 3 for symbols! The points represent the summation over the angular bins (bins not covered by measurements are taken from the fit), the solid line represents our fit. The errors are dominantly due to uncertainties in the normalization.

$A_{3/2}/A_{1/2}$ and the product $P_{in/out} = \Gamma_{\gamma p \rightarrow N^*} \Gamma_{N^* \rightarrow \eta p}$, normalized to this product for the resonance $N(1535)S_{11}$. The errors are estimated from a large number of fits in which the number of resonances, their parametrization, and the relative weight of the different data sets is changed.

We now test the significance of the $N(2080)D_{15}$. Omitting this resonance changes χ^2 by 220 for the data of Fig. 3. Replacing the J^P assignment from $5/2^-$ to $1/2^\pm, \dots, 9/2^\pm$, χ^2 deteriorates in most cases by more than 100. Based on experience with a large number of fits, we do not exclude $J^P = 3/2^-$ ($\Delta\chi^2 = 59$), $1/2^+$ ($\Delta\chi^2 = 73$) or $5/2^+$ ($\Delta\chi^2 = 91$). However, a $N(2080)D_{15}$ is the preferred solution. We do not find evidence for a third S_{11} resonance for which claims are reported at a mass of 1780 MeV [24] or at 1846 MeV [25].

The differential cross sections were integrated to determine the total cross section (Fig. 4). The extrapolation to forward and backward angles uses the result of the isobar analysis. The solid line represents the integration of the partial wave solution.

We have reported a measurement of the total and differential cross sections for photoproduction of η mesons off protons over a wider range, in energy and in production angles, than covered by existing data. An isobar analysis of the data which includes various other data sets determines $N\eta$ couplings of six N^* resonances and uncovers evidence for a new resonance, the $N(2080)D_{15}$.

Acknowledgements

We would like to thank the technical staff of the ELSA machine group and of all the participating institutions for their invaluable contributions to the success

of the experiment. We acknowledge financial support from the Deutsche Forschungsgemeinschaft (DFG). The collaboration with St. Petersburg received funds from DFG and the Russian Foundation for Basic Research. B. Krusche acknowledges support from Schweizerischer Nationalfond. U. Thoma thanks for an Emmy Noether grant from the DFG. A.V. Anisovich and A. Sarantsev acknowledge support from the Alexander von Humboldt Foundation. This work comprises part of the PhD thesis of O. Bartholomy.

- [1] T. Nakano *et al.* [LEPS Collaboration], Phys. Rev. Lett. **91** (2003) 012002.
- [2] V. V. Barmin *et al.* [DIANA Collaboration], arXiv:hep-ex/0304040.
- [3] S. Stepanyan *et al.* [CLAS Collaboration], arXiv:hep-ex/0307018.
- [4] J. Barth *et al.* [SAPHIR Collaboration], Phys. Lett. B **572** (2003) 127.
- [5] C. Alt *et al.* [NA49 Collaboration], arXiv:hep-ex/0310014.
- [6] K. Hagiwara *et al.* [Particle Data Group Collaboration], Phys. Rev. D **66** (2002) 010001.
- [7] S. Capstick and N. Isgur, Phys. Rev. D **34** (1986) 2809.
- [8] L. Y. Glozman, W. Plessas, K. Varga and R. F. Wagenbrunn, Phys. Rev. D **58** (1998) 094030.
- [9] U. Löring, B. C. Metsch and H. R. Petry, Eur. Phys. J. A **10** (2001) 395, 447.
- [10] R. D. Young, D. B. Leinweber, A. W. Thomas and S. V. Wright, Nucl. Phys. Proc. Suppl. **109A** (2002) 55.
- [11] D. G. Richards, M. Gockeler, P. E. Rakow, R. Horsley, C. M. Maynard, D. Pleiter and G. Schierholz, [UKQCD Collaboration], arXiv:nucl-th/0206049.
- [12] N. Kaiser, P. B. Siegel and W. Weise, Phys. Lett. B **362**, 23 (1995).
- [13] A. Anisovich *et al.*, in preparation
- [14] B. Krusche *et al.*, Phys. Rev. Lett. **74** (1995) 3736.
- [15] S. A. Dytman *et al.*, Phys. Rev. C **51** (1995) 2710.
- [16] L. Soezueer *et al.*, <http://gwdac.phys.gwu.edu>.
- [17] F. Renard *et al.* [GRAAL Collaboration], Phys. Lett. B **528** (2002) 215.
- [18] M. Dugger *et al.* [CLAS Collaboration], Phys. Rev. Lett. **89** (2002) 222002 [Erratum-ibid. **89** (2002) 249904].
- [19] E. Aker *et al.* [Crystal Barrel Collaboration], Nucl. Instrum. Meth. A **321** (1992) 69.
- [20] V. Credé *et al.* [CB-ELSA Collaboration], Photoproduction of neutral pions off the proton, in preparation.
- [21] R. Arndt, W. Briscoe, I. Strakovsky and R. Workman, Phys. Rev. C **66** (2002) 055213.
- [22] W. T. Chiang, S. N. Yang, D. Drechsel and L. Tiator, PiN Newslett. **16** (2002) 299 and refs therein.
- [23] D. Rebreyend [GRAAL Collaboration], Nucl. Phys. A **663**, 436 (2000).
- [24] B. Saghai and Z. Li, arXiv:nucl-th/0305004.
- [25] G. Y. Chen, S. Kamalov, S. N. Yang, D. Drechsel and L. Tiator, arXiv:nucl-th/0210013.